Cell-Surface-Associated Tissue Transglutaminase Is a Target of MMP-2 Proteolysis†

Alexey M. Belkin,*,‡,§ Evgeny A. Zemskov,‡,§ Jun Hang,‡ Sergey S. Akimov,‡ Sergey Sikora,|| and Alex Y. Strongin||

Department of Biochemistry, The Holland Laboratory, American Red Cross, Rockville, Maryland 20855, and The Burnham Institute, La Jolla, California 92037

Received April 13, 2004; Revised Manuscript Received July 6, 2004

ABSTRACT: MT1-MMP, a prototypic member of a membrane-type metalloproteinase subfamily, is an invasion promoting protease and an activator of MMP-2. In addition, MT1-MMP proteolysis regulates the functionality of cell-surface adhesion/signaling receptors including tissue transglutaminase (tTG). tTG is known to serve as an adhesion coreceptor for $\beta1/\beta3$ integrins and as an enzyme that catalyzes the cross-linking of proteins and the conjugation of polyamines to proteins. Here, we report that MMP-2, functioning in concert with MT1-MMP, hydrolyzes cell-surface-associated tTG, thereby further promoting the effect initiated by the activator of MMP-2. tTG, in return, preferentially associates with the activation intermediate of MMP-2. This event decreases the rate of MMP-2 maturation and protects tTG against proteolysis by MMP-2. Our cell culture, in vitro experiments, and in silico modeling indicate that the catalytic domain of MMP-2 directly associates with the core enzymatic domain II of tTG (the $K_d = 380$ nM). The follow-up cleavage of the domain II eliminates both the receptor and the enzymatic activity of tTG. Our data illuminate the coordinated interplay involving the MT1-MMP/MMP-2 protease tandem in the regulation of the cell receptors and explain the underlying biochemical mechanisms of the extensive tTG proteolysis that exists at the normal tissue/tumor boundary. Our findings also suggest that neoplasms, which express functionally active MT1-MMP and, therefore, activate soluble MMP-2, can contribute to the degradation of tTG expressed in neighboring host cells. The loss of adhesive and enzymatic activities of tTG at the interface between tumor and normal tissue will decrease cell-matrix interactions and inhibit matrix cross-linking, causing multiple pathological alterations in host cell adhesion and locomotion.

Current evidence suggests that individual members of the matrix metalloproteinase (MMP)[1] family play an important role in the pathological proteolysis of the extracellular matrix and subsequent tissue remodeling (*1*−*3*). The elevated expression of MMPs in neoplasms is frequently associated with invasion by malignant cells, and metastasis and neovascularization of tumors (*3*, *4*).

It has been well-established that membrane type-1 matrix metalloproteinase (MT1-MMP) is a membrane activator of the secretory soluble MMP-2 (Gelatinase A) (*5*−*7*). Because of its destructive capability, the activity of MMP-2 is tightly controlled by multiple regulatory proteins and TIMP inhibitors at the levels of gene expression, proenzyme activation, and enzyme activity and by the clearance of the protease from the extracellular milieu (*4*, *8*−*11*).

MT1-MMP has also been shown to cleave cell-surface-associated adhesion and signaling receptors such as tissue transglutaminase (tTG; protein-glutamine γ-glutamyltransferase, EC 2.3.2.13), CD44, and the precursors of certain α integrin subunits (*12*−*15*). Cell-surface tTG catalyzes covalent cross-linking between reactive lysine and glutamine residues of protein polymers (*16*, *17*). Enzymatic substrates of tTG include collagen, fibrin, β-amyloid, tau, huntingtin, and several other proteins (*18*, *19*). tTG is the key player in celiac disease (*20*). Recently, tTG was found to promote integrin-dependent adhesion and spreading of cells on fibronectin (Fn) and to function as a coreceptor for β_1 and β_3 integrins (*21*−*23*). tTG inhibits tumor growth (*24*) and is expressed as a host response to tumor invasion (*25*). Cell-surface tTG is involved in migration of macrophages on Fn (*22*) and transendothelial migration of $CD8^+$ T lymphocytes (*26*). The enhancement of integrin-mediated adhesion and spreading of cells on Fn is independent of the enzymatic activity of surface tTG. Expression of tTG correlates inversely with the aggressiveness and metastatic potential of tumors, suggesting proteolysis of tTG by MMPs, which are frequently overexpressed in malignant cells (*3*). Proteolysis of tTG at the normal tissue/tumor boundary was observed in invasive tumors (*27*), and in agreement, MT1-MMP was demonstrated to proteolyze tTG in vitro as well as in cultured cancer cells (*13*).

† This work was supported by National Institutes of Health Grants GM62895 (to A.M.B.), CA83017, and CA77470, California Breast-Cancer Research Program Grant 5JB0094, and Susan G. Komen Breast Cancer Foundation Grant 9849 (all to A.Y.S.).

* To whom correspondence should be addressed: Department of Biochemistry, the Holland Laboratory, American Red Cross, 15601 Crabbs Branch Way, Rockville, MD 20855. Telephone: 301-738-0725. Fax: 301-738-0794. E-mail: belkina@usa.redcross.org.

‡ American Red Cross.

§ Present address: Department of Biochemistry and Molecular Biology, University of Maryland School of Medicine, Baltimore, Maryland 21201.

|| The Burnham Institute.

[1] Abbreviations: FBS, fetal bovine serum; Fn, fibronectin; FXIIIA, subunit A of blood coagulation factor FXIII; MMP, matrixmetalloproteinase; MT-MMP, membrane-type MMP; tTG, tissue transglutaminase; TIMP-1 and TIMP-2, tissue inhibitors of metalloproteinase-1 and -2; PAGE, polyacrylamide gel electrophoresis; HT, HT1080.

10.1021/bi049266z CCC: $27.50
Published on Web 08/24/2004

Here, we report that tTG is also a target of MMP-2 proteolysis. Our results indicate that the activator MT1-MMP protease and the activated MMP-2 enzyme work in concert to control the functional activity of cell-surface tTG. These findings shed additional light on the functional interplay between the MT1-MMP/MMP-2 proteolytic system and the target adhesion/signaling receptors.

EXPERIMENTAL PROCEDURES

Proteins, Antibodies, and Cell Lines. The tTG protein was purified from human red blood cells. A potent wide-range inhibitor of MMPs *N*-[(2*R*)-2(hydroxamidocarbonylmethyl)-4-methylpentanoyl]-L-tryptophan methylamide (GM6001 or Ilomastat), tissue inhibitors of metalloproteinases TIMP-1 and TIMP-2, and the individual catalytic domain of MT1-MMP were purchased from Chemicon (Temecula, CA). Anti-β_1 integrin monoclonal antibody 9EG7 and sulfo-NHS-biotin were from Pharmingen (San Diego, CA) and Pierce (Rockford, IL), respectively. Vector- and MT1-MMP-transfected human fibrosarcoma HT1080 and breast carcinoma MCF7 cell lines were selected and maintained as described previously (*11*, *15*, *28*). Rabbit polyclonal antibody against the full-length tTG protein and a monoclonal antibody 4G3 to tTG were characterized earlier (*23*). The purified 42-kDa tTG-binding fragment of Fn, consisting of modules $I_6II_{1,2}I_{7-9}$, was kindly provided by Dr. K. Ingham (American Red Cross). An antibody (H-76) to the receptor of FGF (FGF-R1) was obtained from Santa Cruz Biotechnology (Santa Cruz, CA). TIMP-2-free pro-MMP-2 was isolated from conditioned medium of p2AHT2A72 cells, which were derived from fibrosarcoma HT-1080 cells sequentially transfected with E1A and MMP-2 cDNAs (*5*).

Proteolysis of tTG in Vitro. The MMP-2 latent zymogen was activated for 30 min at 4 °C with *p*-aminophenylmercuric acetate (1 mM). Purified tTG (1−5 μg) was incubated with the individual catalytic domain of MT1-MMP and MMP-2 (0.1−0.3 μg each) for 0.5−12 h at 37 °C in 0.05 M Tris-HCl buffer at pH 7.5, containing 50 mM NaCl, 1 mM $CaCl_2$, and 10 μM $ZnCl_2$. The digest samples were analyzed by SDS−PAGE in 12% gels.

Flow Cytometry. To quantify cell-surface tTG, live, nonpermeabilized cells were co-incubated for 2 h at 37 °C both with and without GM6001 (20 μM), TIMP-1, and TIMP-2 (1 μg/mL each) and then stained with a rabbit affinity-purified polyclonal antibody against tTG (10 μg/mL) and, next, with secondary fluorescein-conjugated IgG. Cells were analyzed by a FACScan flow cytometer (Becton Dickinson). No fewer than three independent experiments were performed on each cell line.

Measurement of the tTG Enzymatic Activity. The enzymatic activity of cell-surface-associated tTG was determined as reported earlier (*21*). Cells (2×10^6) were detached by EDTA and then resuspended in PBS (0.5 mL), containing 2 mM $CaCl_2$ and 10 mg/mL *N*,*N*-dimethylcaseine. The cells were then incubated for 1 h at 37 °C with 10 μCi of [^{3}H]-putrescine (35.7 Ci/mmol, Perkin−Elmer Life Sciences). To evaluate the incorporation of [^{3}H]putrescine, *N*,*N*-dimethylcaseine was precipitated from cell-free supernatants with 10% trichloroacetic acid. Excess label was removed by successively washing the pellets with 5% trichloroacetic acid, ethanol, and acetone. The pellets were dried and redissolved in 1% SDS. Protein-incorporated radioactivity was determined by scintillation counting.

Table 1: Deletion Constructs of tTG[a]

construct	direct primer	reverse primer
tTG16−687	A	B
tTG1−592	C	D
tTG141−687	E	B
tTG461−687	F	B
tTG1−140	C	G
tTG1−460	C	H

[a] Sequences of the A−H primers are 5′-ATCGAAGCTTATGACCAATGGCCGAGACCACCACACGG-3′, 5′-ATCGCTCGAGGGCGGGGCCAATGATGACATTCC-3′, 5′-ATCGAAGCTTACCATGGCCGAGGAGCTGGTCTTAGAGAGG-3′, 5′-ATCGCTCGAGCCGGATCTTGATTTCTGGATTCTCCAGG-3′, 5′-ATCGAAGCTTATGGCCTGGTGCCCAGCGGATGCTGTGTACC-3′, 5′-ATCGAAGCTTATGCACCTGAACAAACTGGCCGAGAAGG-3′, 5′-ATCGCTCGAGGTTGAAGAGCAAAATGAAGTGGCCC-3′, and 5′-ATCGCTCGAGGTTCGCCCTTGTGAAGGCCTCCCTC-3′, respectively.

Binding of the 42-kDa Fragment of Fn to Cells. Cells were detached by EDTA and resuspended in 200 μL of Tyrode's buffer at pH 7.4 (10 mM HEPES, 150 mM NaCl, 2.5 mM KCl, 2 mM $NaHCO_3$, 2 mM $MgCl_2$, 2 mM $CaCl_2$, 1 mg/mL BSA, and 1 mg/mL dextrose). Cells were incubated for 1 h at 37 °C with a 1 μM ^{125}I-labeled 42-kDa Fn fragment (specific activity = 1.6×10^6 cpm/μg). Cells were next layered on 0.5 mL of 20% sucrose in Tyrode's buffer and centrifuged for 5 min at 10 000 rpm. Radioactivity associated with the cell pellet was quantified in a γ counter. Measurements were performed 3 times. Values were corrected for nonspecific binding determined in the presence of excess (10 μM) unlabeled 42-kDa Fn fragment.

Deletion Mutants of tTG. The human tTG cDNA, expressed in the pcDNA3.1myc-HisA/neo vector (Invitrogen, Carlsbad, CA), was used as a template to generate the deletion mutants. The deletion mutants of tTG were generated by the PCR amplification of the tTG sequence employing the oligonucleotide primers shown in Table 1. The following deletion mutants were prepared: the tTG16−687 construct with the deleted N-terminal tail extension, the tTG1−592 construct missing domain IV, and the tTG141−687 construct missing domain I. We also constructed three constructs that code for the individual domains of tTG, such as the tTG461−687 construct that encodes the domains III and IV, the tTG1−140 construct that encodes domain I, and the tTG1−460 construct that encodes domains I and II. After PCR amplification, the constructs were excised with *Hind*III and *Pme*I endonucleases and inserted into the pGene-hygro vector (Invitrogen) for the subsequent transfection and inducible expression of the tTG variants in glioma U251 cells. All of the subcloned cDNA fragments retained the myc/His tag.

Expression of the tTG Constructs in Glioma U251 Cells. Glioma U251 cells, transfected with the pcDNA3.1-neo plasmid bearing the MT1-MMP gene (U-MT cells) and, therefore, stably expressing MT1-MMP, were isolated and extensively characterized earlier (*13*, *28*). In this study, U-MT cells were sequentially transfected, using Lipofectamine 2000 (Gibco-Invitrogen), with the pSwitch-zeo plasmid (Invitrogen) and with the pGene-hygro vector encoding either the subunit A of blood coagulation factor FXIIIA (*21*) or the individual tTG constructs. The transfected cells were grown for 3 weeks in media supplemented with 200 μg/mL neomycine, and hygromycine and zeocine (100 μg/mL each)

to select stable clones. A total of 5−10 isolated individual clones were pooled to generate the cell lines, which were used in our assay. To induce expression of tTG and FXIIIA, cells grown in DMEM−10% FBS were treated with mifepristone (0.1 nM) for 24 h. After the mifepristone treatment, cells were lysed in a RIPA buffer (50 mM Tris-HCl at pH 7.5, containing 1% Triton X-100, 0.5% Na deoxycholate, 0.1% SDS, 150 mM NaCl, 0.5 mM phenylmethylsulfonyl fluoride, 0.5 mM benzamidine, 10 μg/mL leupeptin, and 10 μg/mL aprotinin). Aliquots (50 μg of total cell protein each) were separated by SDS−electrophoresis in 14% acrylamide gel and analyzed by Western blotting with a monoclonal anti-myc 9E10 antibody (1 μg/mL) (Upstate Biotechnology, Chicago, IL), followed by goat anti-mouse IgG conjugated with horseradish peroxidase and a SuperSignal West Pico Chemiluminescent substrate (Pierce).

MMP-2 Binding to tTG. Wells of a 96-well plate were coated with BSA or tTG (10 mg/mL). After blocking of wells with 10% BSA, the MMP-9- and MMP-2-containing serum-free medium samples (150 mL each), conditioned by MT1-MMP-transfected HT-1080 fibrosarcoma cells (HT-MT cells), were added to the wells. After incubation for 1 h at 37 °C, unbound material was removed by washing the wells with 50 mM Tris-HCl buffer at pH 7.5, containing 150 mM NaCl and 0.1% Triton X-100. Bound material was solubilized with 25 mM Tris-2% SDS at pH 7.0 and analyzed by gelatin zymography.

Coprecipitation Studies. To analyze the association of MMP-2 with tTG and β_1 integrins, HT1080 cells expressing MT1-MMP, were lysed in RIPA buffer. Cells were then lysed in a RIPA buffer. β_1 integrins, FGF receptor (FGF-R), and tTG were immunoprecipitated with the monoclonal antibody P4C10, polyclonal antibody to FGF-R, and a rabbit polyclonal anti-tTG antibody from the aliquots (0.5 mg of total protein) of the RIPA lysates, respectively. Similarly, to evaluate the association of MMP-2 with the tTG constructs expressed in U-MT cells, the cells, following a 24-h stimulation with mifepristone (0.1 nM), were lysed in a RIPA buffer and the cell lysates were immunoprecipitated with the monoclonal anti-myc 9E10 antibody and Protein G-Agarose beads (Pierce). The precipitated material was analyzed by gelatin zymography in 0.1% gelatin−10% acrylamide gels (Novex, San Diego, CA).

Immunoprecipitation of Cell-Surface-Associated tTG. U-MT cells were also stably transfected with the original pcDNA3.1-hygro plasmid (vector control), the pcDNA3.1-hygro plasmid bearing the wild-type tTG, and an anti-sense tTG construct. The structure of our anti-sense tTG construct was described earlier (*22*). Transfected cells were selected in the presence of neomycine (200 μg/mL) and hygromycine (100 μg/mL each). Prior to immunoprecipitation assays, cells were co-incubated for 2 h with GM6001 (20 μM) to inhibit the MT1-MMP activity. Further, cells were surface-labeled with membrane-impermeable sulfo-NHS-biotin (0.2 mg/mL) and lysed in a RIPA buffer. tTG was immunoprecipitated from the lysates of surface-biotinylated cells with the affinity-purified polyclonal anti-tTG antibody. The immunoprecipitates were separated by SDS−PAGE and transferred to a membrane, and biotin-labeled tTG was detected with NeutrAvidin conjugated with horseradish peroxidase and a SuperSignal West Pico Chemiluminescent substrate (Pierce).

Analysis of MMP-2 Maturation in Glioma U251 Cells Coexpressing MT1-MMP with tTG. U-MT cells transfected with the original pcDNA3.1-hygro plasmid (vector control), the pcDNA3.1-hygro plasmid bearing the wild-type tTG, and an anti-sense tTG construct (1×10^5 cells each) were incubated for 0.5−6 h in DMEM supplemented with 0.05% BSA. Aliquots (10 μL each) of conditioned medium were analyzed for the gelatinolytic activity of MMP-2 by gelatin zymography.

Analysis of the Interaction Between tTG and MMP-2 by Surface Plasmon Resonance. Purified MMP-2 (20 μg/mL) was covalently coupled by *N*-hydroxysuccinimide to a carboxymethyl dextran (CM5) sensor chip at a density of 500−1000 responsive units (RU) following the recommended procedure of the manufacturer. Binding assays were performed in a Biacore 3000 (BIAcore AB, Uppsala, Sweden). Purified human red blood cell tTG (96−2048 nmol) diluted in HBS-P buffer (0.01 HEPES at pH 7.4, containing 0.15 M NaCl and 0.01% Tween 20) was applied to the chip at a 10 μL/min flow rate. The bound tTG was dissociated from the chip by passing HBS-P buffer, without tTG, for the next 6 min at the same flow rate. For the competition experiments, tTG and the 42-kDa fragment of Fn were diluted to the concentration of 0.5 and 2 μM, respectively, and used individually and jointly to associate the immobilized MMP-2. All binding experiments were performed at 25 °C. Regeneration of the sensor chip surface was performed with 20 μL of 2 M NaCl and 20 mM glycine buffer at pH 9.5. The equilibrium dissociation constant (K_d) was determined from the rate of dissociation/association using the BIAevaluation software program 3.1 (BIAcore AB) and the obtained sensograms.

Structural Analysis. Structural representation and solvent-accessibility analyses of tTG (PDB accession code 1KV3) were performed using the Swiss PDB Viewer (version 3.7, http://www.expasy.org/spdbv). The domain-composition analysis of tTG was performed using PFAM (http://www.sanger-.ac.uk/Software/Pfam), FFAS (http://ffas.ljcrf.edu), and 3D-PSSM (http://www.sbg.bio.ic.ac.uk/∼3dpssm).

Protein−Protein Docking. Protein−protein docking of MMP-2 (PDB accession code 1QIB) to tTG was performed using GRAMM (version 1.03, SUNY at Stony Brook, NY) with the following parameters: helix mode, grid step 1.7, repulsion 10, and angle of rotation −10°. The top five conformations with the highest energy score were analyzed and validated. The top-scored MMP-2•tTG docking model has an energy score of −451, which is comparable with the score of efficiently interacting heterodimer proteins (*29*, *30*).

RESULTS

MMP-2 Cleaves and Inactivates Cellular tTG. After stable transfection with MT1-MMP, human fibrosarcoma HT1080 cells (HT-MT cells) express high levels of this membrane-tethered protease and efficiently activate secretory MMP-2 (Figure 1A). Flow cytometry analyses demonstrated the presence of low amounts of cell-surface tTG in HT-MT cells (Figure 1B) (*13*). Co-incubation with a broad-range hydroxamate inhibitor of MMPs, GM6001 (20 μM), caused a 5-fold increase of the levels of tTG as well as the full inhibition of MMP-2 activation in HT-MT cells. Similarly, if added to HT-MT cells, TIMP-2 (1 μg/mL), a highly potent inhibitor of both MT1-MMP and MMP-2, blocked activation of

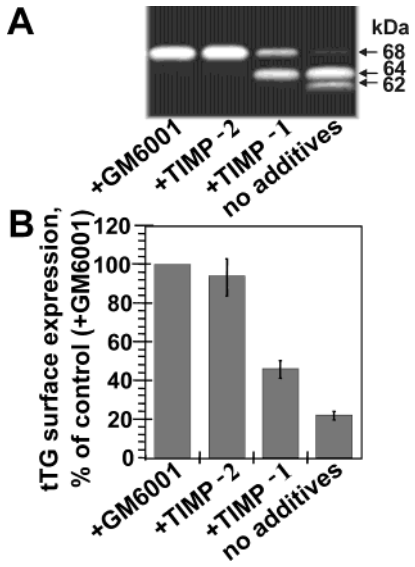

FIGURE 1: Both MT1-MMP and MMP-2 cleave cell-surface-associated tTG. (A) Activation of endogenous MMP-2 by MT1-MMP in human fibrosarcoma HT1080 cells stably transfected with MT1-MMP (HT-MT cells). A zymogram shows conversions of the proenzyme (68 kDa) into the intermediate (64 kDa) and the mature (62 kDa) forms of MMP-2 in the growth medium conditioned by HT-MT cells. The activation of MMP-2 by MT1-MMP is blocked by a hydroxamate inhibitor GM6001 (20 μM) and TIMP-2 (1 μg/mL), while TIMP-1 (1 μg/mL), which is a poor inhibitor of MT1-MMP and a potent inhibitor of MMP-2, predominantly inhibited the autolytic conversion of the MMP-2 intermediate into the mature MMP-2 enzyme. (B) TIMP-1-sensitive MMP-2 contributes to the cleavage of cell-surface-associated tTG in HT-MT cells. HT-MT cells were co-incubated with GM6001 (20 μM), TIMP-1 and TIMP-2 (1 μg/mL each) or left untreated. Live nonpermeabilized cells were next stained with a polyclonal antibody against tTG followed by the staining with the secondary fluorescein-conjugated IgG. The residual levels of cell-surface-associated tTG were identified by flow cytometry of the stained cells.

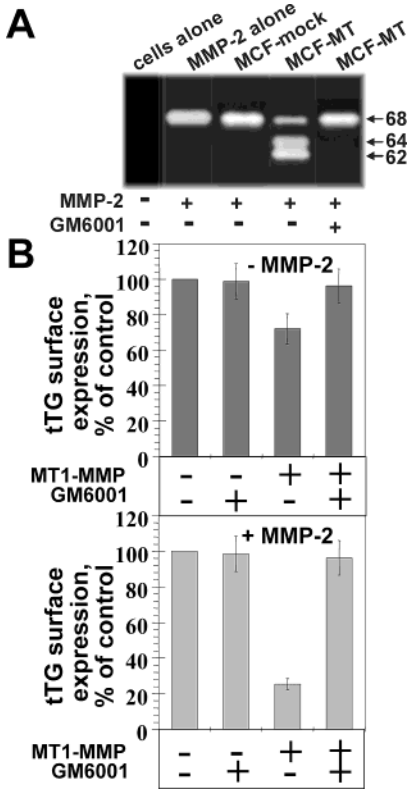

FIGURE 2: MMP-2 amplifies MT1-MMP-dependent proteolysis of tTG. (A) Activation of exogenous MMP-2 by MT1-MMP in human breast MCF7 carcinoma cells lacking or expressing MT1-MMP. A zymogram shows no endogenous MMP-2 in these cells and activation of exogenous MMP-2 by MCF-MT but not by MCF-mock cells. Arrows on the right mark proenzyme (68 kDa), intermediate (64 kDa), and mature (62 kDa) forms of MMP-2. (B) Levels of tTG on the surface of MCF-mock and MCF-MT cells incubated with or without 10 μg/mL MMP-2 and 20 μM GM6001 were determined by staining live, nonpermeabilized cells with polyclonal anti-tTG antibody and flow cytometry. They were expressed as 100% for MCF-mock cells in the absence of GM6001.

MMP-2 and elevated the cell-surface expression of tTG. In contrast, the treatment of HT-MT cells with TIMP-1 (1 μg/mL), which is a poor inhibitor of MT1-MMP but a potent inhibitor of MMP-2, partially restored the levels of tTG in HT-MT cells. In agreement, TIMP-1 partially suppressed the activation of MMP-2 by HT-MT cells and stimulated the predominant accumulation of the 64-kDa activation intermediate of MMP-2 rather than the fully mature 62-kDa enzyme (Figure 1A). These findings indicate that MT1-MMP, resistant to TIMP-1 inhibition, strongly contributes to the proteolysis of cell-surface-associated tTG in HT-MT cells. The differential between the effect of TIMP-2 and TIMP-1, however, suggests a potential additional role of MMP-2 in the proteolysis of cell-surface-associated tTG in HT-MT cells. Because HT-MT cells express high MT1-MMP activity, which itself cleaves tTG, and naturally produce the significant amounts of MMP-2, which is activated by MT1-MMP, it is difficult to specifically define the contributions of the individual proteases in the degradation of tTG in HT-MT cells.

To identify a direct role of MMP-2 in the proteolysis of cellular tTG, we used breast carcinoma MCF7 cells (Figure 2A). We purposefully selected these cells for our experiments because MCF7 cells are strongly deficient in both MMP-2 and MT1-MMP. After stable expression of MT1-MMP, the resulting transfectants (MCF-MT cells) acquired the ability to efficiently activate the external MMP-2 proenzyme. Similar to the parental MCF7 cells, transfectants with the original vector (MCF-mock cells) were incapable of MMP-2 activation. GM6001 (10 μM) fully blocked the activation of external MMP-2 in MCF-MT cells (Figure 2A). Consistent with our earlier data and with the important role of MT1-MMP in the cleavage of tTG, the levels of cell-surface-associated tTG were approximately 30% lower in MCF-MT cells when compared with those in MCF-mock cells (upper panel of Figure 2B). Co-incubation of MCF-MT cells with GM6001 (20 μM) restored the expression of tTG to the levels observed in the MCF-mock cells. To identify the role of MMP-2 in the degradation of tTG, MCF-mock and MCF-MT cells were co-incubated with MMP-2 (lower panel of Figure 2B). The levels of tTG were then determined by flow cytometry. Activation of MMP-2 by MCF-MT cells correlated with a sharp decrease in the cell-surface tTG. In contrast, MMP-2 did not affect tTG in MCF-mock cells, which failed to activate the latent zymogen. GM6001 (20 μM) reversed the effect of MMP-2 in MCF-MT cells and restored the levels of tTG to those seen in MCF-mock control cells. These data suggest that in our cell system the activated MMP-2 enzyme is capable of degrading cell-surface tTG. They indicate that, in MCF-MT cells, MT1-MMP itself degrades ~30% of the surface pool of tTG, while MMP-2 is capable of degrading an additional ~40% of surface tTG.

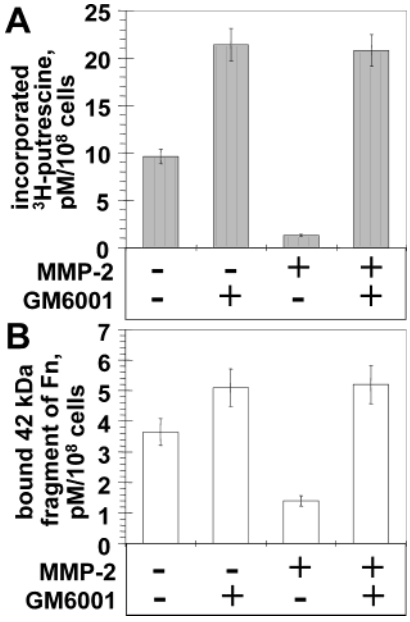

FIGURE 3: Degradation by MMP-2 affects both the enzymatic and adhesive functions of cell-surface-associated tTG. Where indicated, MMP-2 (10 μg/mL) and GM6001 (20 μM) were added to the cells. (A) Enzymatic activity of tTG in MCF-MT cells. The enzymatic activity of tTG expressed on the cell surface was quantified by measuring cell-mediated incorporation of [^{3}H]putrescine into *N,N*-dimethylcaseine. Bars show the means of three individual determinations. (B) Binding of the 42-kDa fragment of Fn to MCF-MT cells in suspension. Cells were preincubated with MMP-2 (10 μg/mL) and GM6001 (20 μM) and then incubated for 1 h at 37 °C with 1 μM ^{125}I-labeled 42-kDa Fn fragment. Cells were separated from excess labeled fragments by centrifugation through a layer of 20% sucrose.

To further support these findings and to demonstrate that MMP-2 proteolysis abolishes the functional activity of surface-associated tTG in MCF-MT cells, we determined both the tTG enzymatic, cross-linking activity and the tTG binding ability to associate with its ligand, the 42-kDa gelatin-binding fragment of Fn (Figure 3). We observed a high level of the tTG enzymatic activity on the surface of untreated MCF-MT cells (Figure 3A). The addition of MMP-2 to the cells strongly suppressed the enzymatic activity of cell-surface-associated tTG. Consistent with its ability to inhibit both MT1-MMP and MMP-2, GM6001 (20 μM) sharply increased the levels of the enzymatic activity of tTG by protecting tTG from the proteolysis. Similar results were obtained in our studies when we tested the ability of MCF-MT cells to bind the 42-kDa Fn fragment in suspension (Figure 3B). Overall, these experimental data tell us that a significant fraction of cell-surface tTG is proteolyzed by the active MMP-2 enzyme in MCF-MT cells and that MMP-2 proteolysis amplifies and extends the proteolysis of tTG by MT1-MMP itself.

Proteolysis of Purified tTG by MMP-2 in Vitro. To extend our findings, we used purified MMP-2 and the enzymatically active individual catalytic domain of MT1-MMP to cleave the purified tTG protein in vitro (Figure 4). Prior to the cleavage experiments, MMP-2 was activated by the *p*-aminophenylmercuric acetate treatment (1 mM at 30 min and 4 °C). The quantitative activation of MMP-2 and the conversion of its inert zymogen into the active enzyme were confirmed by gelatin zymography (data not shown). The catalytic amounts of MT1-MMP and MMP-2 (the enzyme−substrate ratios were in the range of 1:25−100) efficiently and specifically degraded tTG in vitro. The proteolytic fragments of tTG (molecular masses of ~70 and ~41 kDa) generated by MMP-2 were indistinguishable from those observed in the MT1-MMP digest samples. This similarity provides key evidence that the MMP-2 activity is essential for the proteolysis of surface tTG observed in cultured cells. Earlier, the tTG cleavage fragments were partially sequenced to identify the PVP^{375}↓VR, FTR^{458}↓AN, and ANH^{461}↓LN cleavage sites (*13*). Importantly, we had predicted that MT1-MMP cleavage, at any of these three sites, should eliminate both the receptor and enzymatic activity of tTG by separating its NH_2-terminal Fn-binding and the COOH-terminal integrin-binding domains and by inactivating its second (catalytic) domain of tTG. These sequence data are consistent with the results of our enzymatic and Fn-binding studies and confirm that MMP-2 proteolysis inactivates both functional activities of cellular tTG.

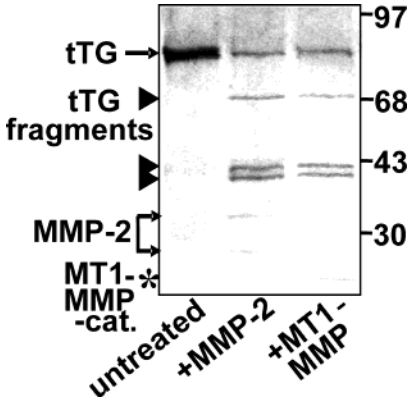

FIGURE 4: Proteolysis of tTG by MMP-2 in vitro. The MMP-2 latent zymogen was activated by *p*-aminophenylmercuric acetate. Purified human red blood cell tTG (5 μg) was incubated for 2 h at 37 °C with MMP-2 (0.2 μg) or with the catalytic domain of MT1-MMP (0.2 μg) in 0.05 M Tris-HCl buffer at pH 7.5, containing 50 mM NaCl, 1 mM $CaCl_2$, and 10 μM $ZnCl_2$. The digest samples were analyzed by SDS−PAGE in 12% gels. The full-length tTG and the tTG cleavage fragments are marked by an arrow and by the arrowheads, respectively. MMP-2 and the catalytic domain of MT1-MMP are marked by a double arrow and an asterisk, respectively. Molecular weight markers are shown on the right.

Direct Binding of MMP-2 to tTG. Next, we evaluated if MMP-2 is capable of directly associating with tTG (Figure 5). For this purpose, we immunoprecipitated tTG, β1 integrins, and the receptor of FGF (FGF-R) from the lysates of HT-MT cells (Figure 5A). The immune complexes were analyzed by gelatin zymography. As expected, no detectable MMP-2 was coprecipitated with the functionally irrelevant FGF-R. The gelatinolytic activity that corresponded to the 64-kDa activation intermediate of MMP-2 was found in both β1 integrin and tTG immunoprecipitates. Because it is well-established that tTG is a coreceptor of β1/β3 integrins (*21*), these observations indicate that secretory MMP-2 is capable of binding directly to cell-surface integrin-associated tTG.

To confirm that the 64-kDa intermediate is predominantly involved in the association with tTG, wells of a 96-well plate were coated with purified tTG (Figure 5B). Then, samples of serum-free medium conditioned by HT-MT cells were incubated with immobilized purified tTG or BSA. These samples contained the proenzyme, the intermediate, and the mature enzyme of MMP-2, as well as the proenzyme and the enzyme of MMP-9. After the incubation, unbound

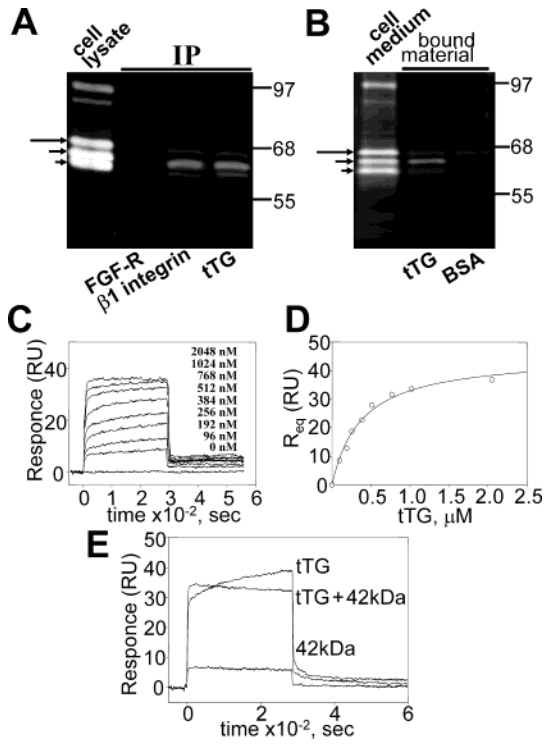

FIGURE 5: MMP-2 directly interacts with tTG. (A and B) MMP-2 associates with tTG in HT-MT cells. The association of MMP-2 with tTG was analyzed by immunoprecipitating (IP) β1 integrin and tTG from the HT-MT cell lysates (A) and by direct binding of MMP-2 to tTG (B) followed by gelatin zymography. (A) HT-MT cells (5×10^6) were lysed in RIPA buffer. FGF-R1, β1 integrin, and tTG were each immunoprecipitated from cell lysates by using the respective antibodies and Protein G-Agarose beads. The immune complexes were analyzed by gelatin zymography to identify coprecipitated MMP-2. (B) Wells of a 96-well plate were coated with BSA (10 mg/mL) and tTG (10 mg/mL). After blocking with 10% BSA, MMP-9- and MMP-2-containing serum-free medium samples (150 mL) conditioned by HT-MT cells (left lane, medium alone) were added to the wells. After incubation for 1 h at 37 °C, unbound material was removed by washing the wells with 50 mM Tris-HCl buffer at pH 7.5, containing 150 mM NaCl and 0.1% Triton X-100. Bound material was solubilized with 25 mM Tris-2% SDS at pH 7.0 and analyzed by gelatin zymography to identify MMP-2. The short, intermediate, and long arrows mark the 62-kDa mature enzyme, the 64-kDa activation intermediate, and the 68-kDa latent proenzyme of MMP-2, respectively. Positions of molecular weight markers are on the right. (C−E) Surface plasmon resonance analysis of the MMP-2·tTG association. Binding of the purified soluble tTG to the immobilized MMP-2 was determined with Biacore 3000. The carboxymethyl dextran sensor chip CM5 was coated with the purified MMP-2 (20 μg/mL) in HBS-P buffer. (C) Association and dissociation of purified tTG (96−2048 nM) with immobilized MMP-2 were monitored in real time while registering the resonance signal (response). (D) Nonlinear regression plot of the response at equilibrium (R_{eq}) versus the concentrations of tTG. The K_d value was calculated using the BIAevaluation software program, version 3.1 (BIAcore AB). (E) Competition experiments. Sensorgrams were generated for the binding of tTG (0.5 μM) and the 42-kDa Fn fragment (2 μM) alone to the immobilized MMP-2. Sensorgrams were also generated for the binding of the preformed tTG·42-kDa Fn fragment complex with the immobilized MMP-2. This complex was formed by co-incubating tTG (0.5 μM) with the excess of the 42-kDa Fn fragment (2 μM) for 10 min on ice. Therefore, the sample was represented by the stoichiometric tTG·42-kDa Fn fragment complex and the free 42-kDa Fn fragment. The samples were injected at 25 °C at a flow rate of 10 μL/min.

material was removed by washing. Bound proteins were solubilized in an SDS−PAGE sample buffer and then analyzed by gelatin zymography. In these experiments, all three forms of MMP-2, the proenzyme, the intermediate, and the mature enzyme were capable of binding collagen (data not shown), but none of the MMP-2 forms associated with BSA. Consistent with our coprecipitation studies (Figure 5A), the 64-kDa intermediate of MMP-2 rather than the proenzyme or the mature enzyme was found most efficient in the tTG binding (Figure 5B).

The binding of MMP-2 to tTG in vitro was also examined using surface plasmon resonance spectroscopy (parts C−E of Figure 5). Purified MMP-2 (a mixture of intermediate and mature forms pretreated with GM6001) was immobilized on the sensor surface. A concentration-dependent saturable binding of tTG (96−2048 nM) to immobilized MMP-2 was observed (Figure 5C). Apparent equilibrium binding constants were determined using the steady-state region of sensograms (Figure 5C). The R_{eq} values were plotted against the total concentration of added tTG, and the data were fit using eq 1 (general fit, steady-state affinity; BIAevaluation 3.1). The equilibrium dissociation constant (K_d) calculated from the ratio k_{off}/k_{on} was 380 nM (Figure 5D). No significant changes in kinetic constants were observed when the flow rate was varied from 2 or 5 μL/min to 10 μL/min.

To extend these findings further, we examined if the ligand of tTG (the 42-kDa fragment of Fn) is capable of competitively inhibiting the tTG·MMP-2 associations. The 42-kDa fragment of Fn alone failed to associate with MMP-2. In agreement, the sample represented by the stoichimetric tTG·, the 42-kDa Fn fragment complex, and a 2-molar excess of the 42-kDa Fn did not significantly affect the binding of MMP-2 to tTG. We infer from these results that distinct domains of tTG are involved in the binding to the 42-kDa Fn fragment and to MMP-2. It has been previously established that the 42-kDa fragment of Fn binds to the NH_2-terminal domain I of tTG (residues 1−140) (*31*). The three MMP cleavage sites are localized within the tTG core domain II (residues 145−460). These data suggest that MMP-2 binds to the tTG region distinct from domain I, possibly to the core (catalytic) domain II of tTG. To gain additional support for this hypothesis, we used the deletion mutants of tTG in the MMP-2-binding assay as well as modeled the MMP-2·tTG interaction by in silico modeling.

Catalytic Domain II of tTG Is Essential for MMP-2 Binding. To identify the individual domain involved in the association of tTG with MMP-2, we used glioma U-MT cells, which had been stably transfected with MT1-MMP and naturally synthesize the high levels of MMP-2 (*13*, *28*). In our current study, U-MT glioma cells were additionally stably transfected with the wild-type tTG and the deletion mutants of tTG. These deletion mutants included the tTG16−687 construct with the deleted N-terminal tail extension, the tTG1−592 construct that was devoid of domain IV, the tTG141−687 construct that missed domain I, the tTG461−687 construct that lacked domains I and II, the tTG1−140 construct that lacked domains II−IV, and finally, the tTG1−460 construct that lacked domains III and IV. The structure of several tTG constructs is illustrated in Figure 6A. We also isolated U-MT cells, which had been stably transfected with subunit A of blood coagulation factor FXIII (FXIIIA), and used this cell line as a control in our assays. All of the constructs were COOH-terminally tagged with a myc tag. The presence of the tag provided us with an opportunity to

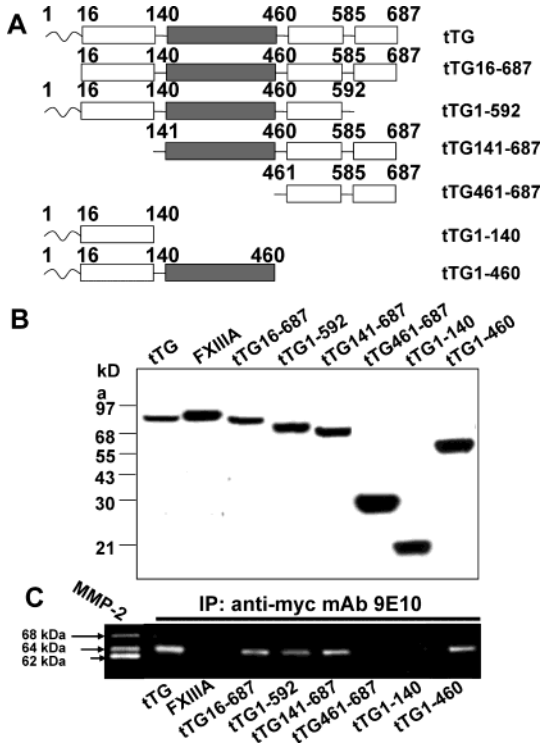

FIGURE 6: tTG binds MMP-2 via the catalytic domain II. (A) Schematic representation of the tTG constructs. The domain size was assigned according to the crystal structure of human tTG (*33*). Domains I, III, and IV are in white, while domain II is shown in gray. All of the constructs contained the C-terminal myc/His tag (not shown). (B) Expression of the tTG and FXIIIA constructs in U-MT cells. After induction of tTG and FXIIIA with mifepristone, cell lysates were analyzed by Western blotting with the monoclonal anti-myc 9E10 antibody. Molecular weight markers are shown on the left. (C) Coprecipitation of cellular tTG with MMP-2. U-MT cells transfected with the tTG and FXIIIA constructs (5×10^6 cells each) were lysed in the RIPA buffer. tTG and FXIIIA were each immunoprecipitated with 9E10 anti-myc mAb from the cell lysates. The immunoprecipitates were analyzed by gelatin zymography to identify coprecipitated MMP-2. MMP-2 alone (no cells) is shown on the left. The short, intermediate, and long arrows point to the 62-kDa mature enzyme, the 64-kDa activation intermediate, and the 68-kDa latent proenzyme of MMP-2, respectively. Note the exclusive association of the activation intermediate of MMP-2 with the tTG constructs, which contain the second (catalytic) domain of tTG.

use anti-myc antibody in our Western blotting tests and pull-down assays. Western blotting with the anti-myc antibody confirmed expression of the tTG and FXIIIA constructs in U-MT cells (Figure 6B). Further, we immunoprecipitated tTG from the cell lysates and employed gelatin zymography to identify MMP-2, which might have coprecipitated with tTG (Figure 6C). These pull-down experiments demonstrated the efficient association of the 64-kDa activation intermediate of MMP-2 with the tTG constructs, which exhibited domain II. In contrast, the constructs missing domain II such as tTG1−140, which represented domain I, and tTG461−687, which represented domains III and IV, were totally incapable of MMP-2 binding. Accordingly, we concluded that the peptide sequence of the core (catalytic) second domain of tTG is essential for the binding of tTG with MMP-2.

Protein−Protein Docking. Because the crystal structures of both MMP-2 and tTG are known (*32*, *33*), we used protein−protein docking to determine the putative role of the core tTG domain peptide sequence in the MMP-2·tTG

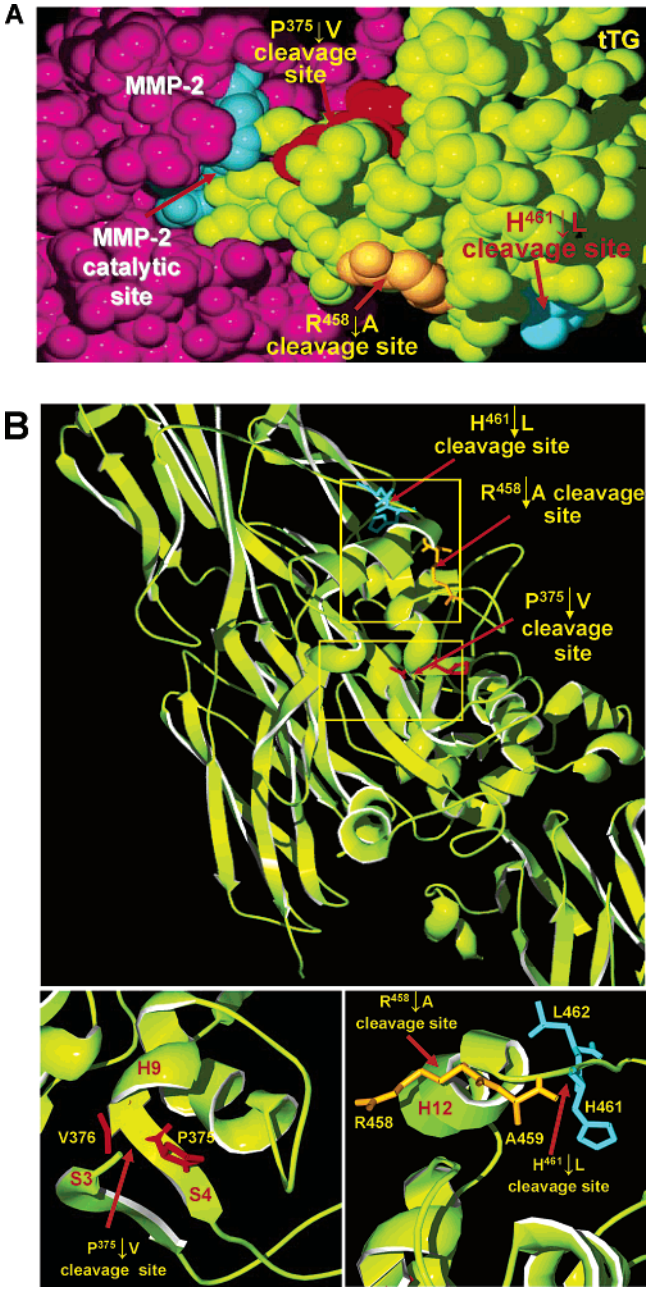

FIGURE 7: MMP-2·tTG interactions. (A) The MMP-2·tTG interaction model. Protein−protein docking was performed using the GRAMM software. The energy score of the docked model is −401. The MMP-2 active-site residues His^{201}, Glu^{202}, His^{205}, and His^{211} are in blue, while the rest of the MMP-2 molecule is in purple. The active site of MMP-2 is in immediate proximity of the P^{375}↓V cleavage site (red) of tTG (green). The cleavage sites R^{458}↓A and H^{461}↓L are shown in orange and blue, respectively. (B) Structural representation of the MMP-2 cleavage sites in tTG. Top panel, the structure of the full-length tTG (green ribbon). MMP-2 cleavage sites H^{461}↓L, R^{458}↓A, and P^{375}↓V are shown in blue, orange, and red, respectively. Bottom panels, close-up of the MMP-2 cleavage sites in tTG.

complex formation (Figure 7). Specifically, we studied the possible binding modes of a tTG monomer (PDB accession code 1KV3) to MMP-2 (PDB accession code 1QIB). Modeling was performed using GRAMM hydrophobic docking software. The five most probable models of the respective complexes were generated. The model with the highest probability scores is shown in Figure 7A. It suggests that the catalytic domain of MMP-2 specifically interacts

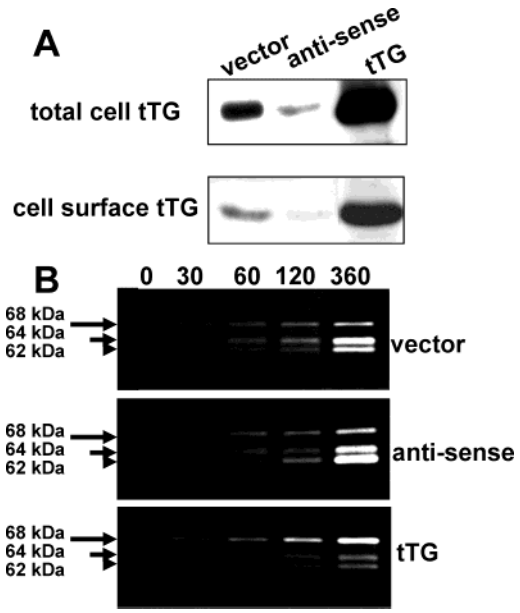

FIGURE 8: Cell-surface tTG inhibits maturation of MMP-2. (A) Expression of total cell tTG (upper panel) and cell-surface-associated tTG (lower panel) in glioma U-MT cells. U-MT cells were stably transfected with the original pcDNA3.1-hygro vector or the pcDNA3.1-hygro vector bearing the wild-type and anti-sense tTG constructs. The levels of total cell and cell-surface-associated tTG were identified by Western blotting as described in the Experimental Procedures. (B) tTG inhibits MMP-2 activation. U-MT cells transfected with the original vector, the wild-type tTG, and the anti-sense tTG construct were incubated for the indicated time in DMEM. Aliquots of conditioned medium were analyzed for the MMP-2 activity by gelatin zymography. The short, intermediate, and long arrows point to the 62-kDa mature enzyme, the 64-kDa activation intermediate, and the 68-kDa latent proenzyme of MMP-2, respectively. Note that tTG inhibits the conversion of the latent form of MMP-2 into the intermediate and the mature enzyme species.

with the core (catalytic) domain II of tTG. The active site of MMP-2 is localized in the immediate proximity of the PVP^{375}↓VR cleavage site. These findings imply, most likely, that MMP-2 initially cleaves the polypeptide sequence of tTG at the PVP^{375}↓VR site. This cleavage is followed by secondary cleavages at the FTR^{458}↓AN and ANH^{461}↓LN sites. These hypotheses correlate well with the in vitro cleavage data, which show the predominant accumulation of the ~41-kDa tTG fragments in the MMP-2 cleavage samples (Figure 4). MMP-2 cleavage at these three sites should eliminate both the receptor and the enzymatic activity of tTG by separating its NH_2-terminal Fn-binding domain I and the COOH-terminal integrin-binding domain IV and by inactivating the core (catalytic) domain II of tTG. The relative positions of these three cleavage sites in the tTG molecule are shown in Figure 7B. In the tTG molecule, the PVP^{375}↓VR cleavage site is localized at the boundary between the antiparallel β-sheet 4 of the E sheet (residues 367−375) and the right-handed α-helix 9 (residues 376−382) of the domain II. The FTR^{458}↓AN cleavage takes place at the C-terminal end of the right-handed α-helix 12 (residues 449−459), while the ANH^{461}↓LN site is located in the unstructured loop region 460−472 connecting the α-helix 12 with the short β-strand 1 (residues 473−478) of the I sheet of domain II.

tTG Inhibits MMP-2 Maturation. To identify the functional role of tTG in MMP-2 activation and maturation, we used U-MT cells coexpressing MT1-MMP with the wild-type tTG and the anti-sense tTG constructs. As expected, transfection of U-MT cells with the wild-type tTG significantly enhanced the expression of tTG relative to that observed in the vector control, while transfection of the cells with the anti-sense construct sharply decreased the levels of the cell surface and total cell expression of tTG in glioma cells (Figure 8A). Further, we evaluated the levels of MMP-2 activation by U-MT cells coexpressing MT1-MMP with the tTG constructs. For these purposes, cells were incubated for 0.5−6 h in serum-free medium. Aliquots of the medium were withdrawn at the indicated time (Figure 8B), and the status of MMP-2 in the samples was identified by gelatin zymography. Activation of MMP-2 was most prominent in the cells expressing the anti-sense tTG, while in the cells overexpressing tTG, the levels of MMP-2 activation were strongly suppressed relative to the vector control. The autolytic conversion of the 64-kDa intermediate into the fully activated mature 62-kDa MMP-2 enzyme rather than the MT1-MMP-dependent conversion of the 68-kDa MMP-2 proenzyme into the activation intermediate is likely to be most affected by tTG. These data correlate well with the efficient binding of tTG with the activation intermediate of MMP-2 (parts A−C of Figure 5). Maturation of MMP-2 is likely to occur in trans and, accordingly, involves two molecules of MMP-2 (*7*, *8*). In agreement, tTG, by binding the MMP-2 activation intermediate rather than the latent zymogen or the fully active enzyme, reduces the clustering of MMP-2 at the cell surface, decreases the rate of MMP-2 maturation, and protects itself from a proteolytic attack by the fully mature MMP-2 enzyme.

DISCUSSION

Invasion-promoting membrane-anchored metalloproteinase MT1-MMP is a key enzyme in cell locomotion (*9*). Current evidence suggests that MT1-MMP operates in many ways in cells and tissues, including direct matrix degradation, proteolytic processing of cell-adhesion/signaling receptors, and the activation of soluble MMPs, such as MMP-2 and MMP-13 (*7*, *34*, *35*). The activated MMP-2 may further promote matrix cleavage and, therefore, increase the matrix proteolysis and tissue remodeling, which are induced by MT1-MMP itself.

Here, we addressed the question: "if MMP-2 works in tandem with MT1-MMP in matrix proteolysis, does it function in a similar way in the proteolytic control of the receptor functionality?" So far, the relative contribution of MMP-2 to the proteolytic degradation of surface receptors, such as tTG (protein-glutamine γ-glutamyltransferase, EC 2.3.2.13), remains unidentified. tTG is a multifunctional protein involved in enzymatic cross-linking and stabilization of matrix proteins and serves as an adhesion coreceptor for β1/β3 integrins. The proper functioning of extracellular tTG is essential for regulation and maintenance of cell−matrix interactions and, in addition, for the locomotion of both malignant and host cells (*13*, *22*, *23*). In contrast, an aberrant functionality of tTG is associated with multiple pathophysiological conditions (*17*).

We demonstrated that MMP-2 is highly efficient both in vitro and in cell-culture conditions in cleaving tTG. MMP-2 predominantly binds with the catalytic core domain II of tTG. In agreement, MMP-2 proteolysis primarily targets this domain of tTG and results in the elimination of the catalytic and adhesion activity of this protein. Our observations suggest that, in cell systems examined in the present study,

MMP-2 is as important as MT1-MMP, in the degradation of surface tTG. These findings provide the underlying biochemical mechanisms of tTG proteolysis frequently observed at the malignant/host cell boundary in aggressive tumors (*27*, *36*). Because tTG inhibits tumor growth and is expressed as a host response to tumor invasion (*25*), the cleavage of this multifunctional protein by ubiquitous soluble MMP-2 is likely to play a significant role in the regulation of cell−matrix interactions, matrix composition, and migration/invasion of the malignant and host cells.

Overall, our studies illustrate a concerted interplay between soluble MMP-2 and its activator, the membrane-tethered MT1-MMP, in regulating the functionality of cell-surface receptors. Our findings support and extend previous observations concerning a functional collaboration between these two proteases. Thus, MT1-MMP degrades a lipoprotein-receptor-related protein LRP that is involved in the clearance of MMP-2 (*37*) and, therefore, stimulates the survival of MMP-2 activity in the extracellular milieu (*11*). The coordinated expression of MT1-MMP and MMP-2 in malignant cells further contributes to a joint rather than an individual effect imposed by these highly potent proteases on the matrix and cell-surface receptors of malignant and host cells.

REFERENCES

1. Coussens, L. M., Fingleton, B., and Matrisian, L. M. (2002) Matrix metalloproteinase inhibitors and cancer: Trials and tribulations, *Science 295*, 2387−2392.
2. Overall, C. M., and Lopez-Otin, C. (2002) Strategies for MMP inhibition in cancer: Innovations for the post-trial era, *Nat. Rev. Cancer 2*, 657−672.
3. Egeblad, M., and Werb, Z. (2002) New functions for the matrix metalloproteinases in cancer progression, *Nat. Rev. Cancer 2*, 161−174.
4. Bauvois, B. (2004) Transmembrane proteases in cell growth and invasion: New contributors to angiogenesis? *Oncogene 23*, 317−329.
5. Strongin, A. Y., Collier, I., Bannikov, G., Marmer, B. L., Grant, G. A., and Goldberg, G. I. (1995) Mechanism of cell surface activation of 72-kDa type IV collagenase. Isolation of the activated form of the membrane metalloprotease, *J. Biol. Chem. 270*, 5331−5338.
6. Seiki, M. (1999) Membrane-type matrix metalloproteinases, *APMIS 107*, 137−143.
7. Murphy, G., Stanton, H., Cowell, S., Butler, G., Knauper, V., Atkinson, S., and Gavrilovic, J. (1999) Mechanisms for pro matrix metalloproteinase activation, *APMIS 107*, 38−44.
8. Hernandez-Barrantes, S., Bernardo, M., Toth, M., and Fridman, R. (2002) Regulation of membrane type-matrix metalloproteinases, *Semin. Cancer Biol. 12*, 131−138.
9. Seiki, M., Mori, H., Kajita, M., Uekita, T., and Itoh, Y. (2003) Membrane-type 1 matrix metalloproteinase and cell migration, *Biochem. Soc. Symp.* 253−262.
10. Lambert, E., Dasse, E., Haye, B., and Petitfrere, E. (2004) TIMPs as multifacial proteins, *Crit. Rev. Oncol. Hematol. 49*, 187−198.
11. Rozanov, D. V., Hahn-Dantona, E., Strickland, D. K., and Strongin, A. Y. (2004) The low-density lipoprotein receptor-related protein LRP is regulated by membrane type-1 matrix metalloproteinase (MT1-MMP) proteolysis in malignant cells, *J. Biol. Chem. 279*, 4260−4268.
12. Kajita, M., Itoh, Y., Chiba, T., Mori, H., Okada, A., Kinoh, H., and Seiki, M. (2001) Membrane-type 1 matrix metalloproteinase cleaves CD44 and promotes cell migration, *J. Cell Biol. 153*, 893−904.
13. Belkin, A. M., Akimov, S. S., Zaritskaya, L. S., Ratnikov, B. I., Deryugina, E. I., and Strongin, A. Y. (2001) Matrix-dependent proteolysis of surface transglutaminase by membrane-type metalloproteinase regulates cancer cell adhesion and locomotion, *J. Biol. Chem. 276*, 18415−18422.
14. Deryugina, E. I., Ratnikov, B. I., Postnova, T. I., Rozanov, D. V., and Strongin, A. Y. (2002) Processing of integrin α(v) subunit by membrane type 1 matrix metalloproteinase stimulates migration of breast carcinoma cells on vitronectin and enhances tyrosine phosphorylation of focal adhesion kinase, *J. Biol. Chem. 277*, 9749−9756.
15. Ratnikov, B. I., Rozanov, D. V., Postnova, T. I., Baciu, P. G., Zhang, H., DiScipio, R. G., Chestukhina, G. G., Smith, J. W., Deryugina, E. I., and Strongin, A. Y. (2002) An alternative processing of integrin α(v) subunit in tumor cells by membrane type-1 matrix metalloproteinase, *J. Biol. Chem. 277*, 7377−7385.
16. Fesus, L., and Piacentini, M. (2002) Transglutaminase 2: An enigmatic enzyme with diverse functions, *Trends Biochem. Sci. 27*, 534−539.
17. Lorand, L., and Graham, R. M. (2003) Transglutaminases: Crosslinking enzymes with pleiotropic functions, *Nat. Rev. Mol. Cell Biol. 4*, 140−156.
18. Andringa, G., Lam, K. Y., Chegary, M., Wang, X., Chase, T. N., and Bennett, M. C. (2004) Tissue transglutaminase catalyzes the formation of α-synuclein crosslinks in Parkinson's disease, *FASEB J. 18*, 932−934.
19. Citron, B. A., Suo, Z., SantaCruz, K., Davies, P. J., Qin, F., and Festoff, B. W. (2002) Protein crosslinking, tissue transglutaminase, alternative splicing, and neurodegeneration, *Neurochem. Int. 40*, 69−78.
20. Reif, S., and Lerner, A. (2004) Tissue transglutaminase—The key player in celiac disease: A review, *Autoimmun. Rev. 3*, 40−45.
21. Akimov, S. S., Krylov, D., Fleischman, L. F., and Belkin, A. M. (2000) Tissue transglutaminase is an integrin-binding adhesion coreceptor for fibronectin, *J. Cell Biol. 148*, 825−838.
22. Akimov, S. S., and Belkin, A. M. (2001) Cell surface tissue transglutaminase is involved in adhesion and migration of monocytic cells on fibronectin, *Blood 98*, 1567−1576.
23. Akimov, S. S., and Belkin, A. M. (2001) Cell-surface transglutaminase promotes fibronectin assembly via interaction with the gelatin-binding domain of fibronectin: A role in TGFβ-dependent matrix deposition, *J. Cell Sci. 114*, 2989−3000.
24. Johnson, T. S., Knight, C. R., el-Alaoui, S., Mian, S., Rees, R. C., Gentile, V., Davies, P. J., and Griffin, M. (1994) Transfection of tissue transglutaminase into a highly malignant hamster fibrosarcoma leads to a reduced incidence of primary tumour growth, *Oncogene 9*, 2935−2942.
25. Haroon, Z. A., Lai, T. S., Hettasch, J. M., Lindberg, R. A., Dewhirst, M. W., and Greenberg, C. S. (1999) Tissue transglutaminase is expressed as a host response to tumor invasion and inhibits tumor growth, *Lab. Invest. 79*, 1679−1686.
26. Mohan, K., Pinto, D., and Issekutz, T. B. (2003) Identification of tissue transglutaminase as a novel molecule involved in human CD8+ T cell transendothelial migration, *J. Immunol. 171*, 3179−3186.
27. Hettasch, J. M., Bandarenko, N., Burchette, J. L., Lai, T. S., Marks, J. R., Haroon, Z. A., Peters, K., Dewhirst, M. W., Iglehart, J. D., and Greenberg, C. S. (1996) Tissue transglutaminase expression in human breast cancer, *Lab. Invest. 75*, 637−645.
28. Deryugina, E. I., Bourdon, M. A., Reisfeld, R. A., and Strongin, A. (1998) Remodeling of collagen matrix by human tumor cells requires activation and cell surface association of matrix metalloproteinase-2, *Cancer Res. 58*, 3743−3750.
29. Vakser, I. A. (1997) Evaluation of GRAMM low-resolution docking methodology on the hemagglutinin-antibody complex, *Proteins* Suppl. *1*, 226−230.
30. Katchalski-Katzir, E., Shariv, I., Eisenstein, M., Friesem, A. A., Aflalo, C., and Vakser, I. A. (1992) Molecular surface recognition: Determination of geometric fit between proteins and their ligands by correlation techniques, *Proc. Natl. Acad. Sci. U.S.A. 89*, 2195−2199.
31. Radek, J. T., Jeong, J. M., Murthy, S. N., Ingham, K. C., and Lorand, L. (1993) Affinity of human erythrocyte transglutaminase for a 42-kDa gelatin-binding fragment of human plasma fibronectin, *Proc. Natl. Acad. Sci. U.S.A. 90*, 3152−3156.
32. Morgunova, E., Tuuttila, A., Bergmann, U., Isupov, M., Lindqvist, Y., Schneider, G., and Tryggvason, K. (1999) Structure of human pro-matrix metalloproteinase-2: Activation mechanism revealed, *Science 284*, 1667−1670.
33. Liu, S., Cerione, R. A., and Clardy, J. (2002) Structural basis for the guanine nucleotide-binding activity of tissue transglutaminase and its regulation of transamidation activity, *Proc. Natl. Acad. Sci. U.S.A. 99*, 2743−2747.
34. Sternlicht, M. D., and Werb, Z. (2001) How matrix metalloproteinases regulate cell behavior, *Annu. Rev. Cell Dev. Biol. 17*, 463−516.

35. Seiki, M., and Yana, I. (2003) Roles of pericellular proteolysis by membrane type-1 matrix metalloproteinase in cancer invasion and angiogenesis, *Cancer Sci. 94*, 569−574.
36. Birckbichler, P. J., Bonner, R. B., Hurst, R. E., Bane, B. L., Pitha, J. V., and Hemstreet, G. P., III (2000) Loss of tissue transglutaminase as a biomaker for prostate adenocarcinoma, *Cancer 89*, 412−423.
37. Yang, Z., Strickland, D. K., and Bornstein, P. (2001) Extracellular matrix metalloproteinase 2 levels are regulated by the low-density lipoprotein-related scavenger receptor and thrombospondin 2, *J. Biol. Chem. 276*, 8403−8408.

BI049266Z